AD-A114 411 STANFORD UNIV CA INST FOR PLASMA RESEARCH F/G 3/2
IUE OBSERVATIONS OF HYADES STARS,(U)
JAN 82 M S ZOLCINSKI, S K ANTIOCHOS N00014-75-C-0673
UNCLASSIFIED SU-IPR-866 NL

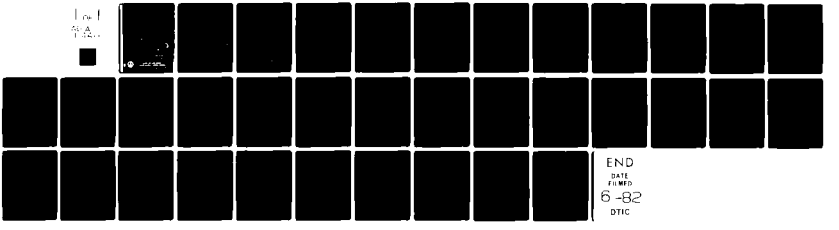

END
DATE FILMED
6-82
DTIC

IUE OBSERVATIONS OF HYADES STARS

by

Marie-Christine S. Zolcinski, Spiro K. Antiochos,
Robert A. Stern and Arthur B.C. Walker

NATIONAL AERONAUTICS AND SPACE ADMINISTRATION
Grant NSG 5131
Grant NSG 5417
Grant NAGW-92
Grant NGR-05-020-668
Grant NGL-05-020-272
Grant NAS 7-100

N00014-75C-0673

SUIPR Report No. 866

January 1982

INSTITUTE FOR PLASMA RESEARCH
Stanford University, Stanford, California

IUE OBSERVATIONS OF HYADES STARS

By

Marie-Christine S. Zolcinski[1], Spiro K. Antiochos[1]
Robert A. Stern[2], Arthur B. C. Walker[1]

Submitted to Astrophysical Journal

(1) Institute For Plasma Research, Stanford University, Stanford, California 94305

(2) Jet Propulsion Laboratory, California Institute For Technology, Pasadena, California 91109

ABSTRACT

We have obtained short wavelength, low dispersion ultraviolet spectra of seven of the brightest X-ray emitting stars in the Hyades cluster with the IUE observatory. Four of the stars show evidence of emission lines characteristic of transition region temperatures (~ 30,000 - 2000,000 K): for the remaining three stars, we derive upper limits for emission line fluxes. In addition, we have observed three of the above stars with the long wavelength spectrograph on IUE at high dispersion and find evidence for chromospheric emission from the MG II h and k lines for two of these objects. Combining the IUE results with X-ray observations from the survey of the Hyades with the Einstein Observatory carried out by Stern et al. (1981), we estimate the differential emission measure function for each of the above stars. We derive constraints on stellar atmospheric parameters (chromospheric pressure, coronal temperature and "filling factor"), and discuss the implications of our results for models of stellar chromospheres and coronae.

Subject headings: clusters: open - stars: chromospheres - ultraviolet: spectra - X-rays: sources

I. INTRODUCTION

Ultraviolet and X-ray observations of the outer atmospheres of cool stars made with the IUE and Einstein satellites have recently led to a major reassessment of theoretical models for stellar chromospheres, transition regions and coronae. Previous X-ray stellar surveys (e.g., Vaiana et al. 1981, Walter and Bowyer 1981, Stern et al. 1981) have indicated that many solar type stars have X-ray luminosities as high as 10^3 times that of the sun. Ultraviolet observations demonstrate that emission line fluxes from many of these same stars are an order of magnitude or more greater than solar (Linsky 1981, Dupree 198k), and that the transition region line fluxes correlate very well with X-ray fluxes (Ayres, Marstad and Linsky 1981).

Stern et al. (1981) have reported on an extensive soft X-ray survey of the central region of the Hyades cluster with Einstein. Their results demonstrate that G dwarfs in the Hyades have typical X-ray luminosities $(L_x) \sim$ 30 times or more than solar. However, the X-ray spectra can only be roughly determined at this time from the Einstein Imaging Proportional Counter data. Thus, in the context of loop models for the corona and transition region, the coronal temperature, area coverage factor, and pressure at the base of the transition region cannot be determined independently. However, far ultraviolet observations of transition region lines, in conjunction with the X-ray measurements, can be used to constrain these parameters.

In this paper, we discuss IUE observations of transition region and chromospheric emission from a group of Hyades dwarfs that are strong X-ray emitters as seen in the Stern et al. (1981) survey. In Section II we describe the observations and compare our results with those from previous IUE observations of cool stars. In Section III we discuss the application of static loop models to our data, and in Section IV we present a brief summary of our work.

II. OBSERVATIONS

The seven selected stars were observed with the short wavelength prime (SWP) camera on IUE at low dispersion (~6 Å resolution from 1175-2000 Å). Three of the seven were also observed with the long wavelength redundant (LWR) camera at high dispersion (~0.2 Å resolution at the Mg II h and k lines near 2800 Å). The design and operation of the IUE satellite is described in Boggess et al. (1978a,b).

The characteristics of the observed stars are listed in Table 1, the observations are summarized in Table 2, and the spectra are illustrated in Figure 1 for the short-wavelength range and Figure 2 for the long-wavelength Mg II h and k lines. All the targets were observed through the IUE aperture (10" x 20"). The extracted spectra were corrected to the revised intensity transfer function according to the algorithm proposed by Holm (1979), and then converted to absolute flux units using the Bohlin et al. (1980) sensitivity curve.

Proposed line identifications are based on the solar line lists of Burton and Ridgeley (1970) and Doschek et al. (1976). The reality of the line features was assessed in a similar manner to that described in Linsky et al. (1979). Emission line fluxes and 2σ upper limits include uncertainties due to stellar continuum and instrumental background. In Table 3 we give the measured line fluxes and upper limits to line fluxes at earth for both the SWP and LWR spectra. We estimate the accuracy of these fluxes to

be better than a factor of 2. Also included in Table 3 are the soft X-ray fluxes from the selected stars (Stern et al. 1981, Zolcinski (1981). Surface fluxes for the four stars in which we detected emission lines, as well as for the quiet sun, are given in Table 4 using the method described by Ayres, Marstad and Linsky (1981), which converts fluxes at earth to stellar surface fluxes by estimating the stellar angular diameter from the color index relation of Barnes and Evans (1976).

a) Short Wavelength Spectra (1175-2000 Å)

Of the three F stars in our observing program 17 Tau (F0 V), BD+15: 640 (F5 V), and 70 Tau (F7 V), all but the earliest, 71 Tau, show evidence for far-ultraviolet line emission. N V λ1240, indicative of gas at a temperature $T \sim 2 \times 10^5$ K, is present only in the spectrum of 70 Tau, although its measured intensity may be suspect because of nearby geocoronal Ly α. C IV λ1549 ($T \sim 1 \times 10^5$ K) is present in both +15: 640 and 70 Tau at about the same level. C II λ1335 ($T \sim 3 \times 10^4$ K) is also easily identifiable in both spectra. Cooler material ($T < 10^4$ K) is indicated by the presence of C I λλ 1561, 1657 in BD+15:640, but is not seen in the 70 Tau spectrum. This is somewhat curious in light of the similarity of BD+15:640 and 70 Tau in spectral type and magnitude: however, this is not inconsistent with the errors inherent in such weak detections.

The complete absence of chromospheric or transition region line emission in the case of 71 Tau is consistent with earlier results on F stars summarized by Linsky (1981), which suggest that most F stars with $B-V \lesssim 0.32$

do not show such line emission. As Linsky points out, however, this is not conclusive proof that early F stars lack transition regions, as the underlying bright UV continuum makes it difficult to observe such emission. Since 71 Tau is the brightest X-ray source detected by Stern et al. (1981), the absence of a transition region appears unlikely.

The SWP spectra of the four G stars, BD+14:693 (G1 V), +16:592 (G1 V), + 15 :598 (G5 V), and + 16 :601 (G6 V), are considerably noisier due to limitations on observing time. Only the G1 dwarfs show evidence of line emission, with C IV λ1549 present at roughly twice the intensity in BD + 14^{o} 693 as in BD + 16^{o} 592. Although the BD + 14 :693 spectrum has many instrumental noise spikes, it is possible to identify line emission due to Si IV λ1394 ($T \sim 8 \times 10^{4}K$), C II λ1335 ($T \sim 3 \times 10^{4}K$), and Si II λ1808, 1817 ($T > 10^{4}K$). The BD + 14 :693 spectrum is particularly interesting in comparison to the solar UV spectrum plotted by Ayres, Marstad and Linsky (1981): in the case of the sun, the Si II blend is twice as strong as C IV, yet in the BD + 14^{o} 693 spectrum, the two sets of lines are of nearly equal strength. This suggests an enhancement of the hotter ($T > 2 \times 10^{4}K$) material relative to that of the chromosphere, as compared to the sun. It is important to note that the absolute flux in the C IV line seen in BD + 14^{o} 693 is about thirty times higher than that of the quiet sun, consistent with the much higher soft X-ray flux seen in BD + 14^{o} 693. The other three stars for which C IV (1540) was observed all appear to be very similar in their C IV and X-ray emission, (Table 4). Although this may be taken as evidence for a definite correlation between soft X-ray and C IV intensity (Ayres, Marstad and Linsky 1981), our data set is too limited to draw any statistically significant conclusions.

We give upper limits only for the line fluxes in BD + 16 : 601 and BD + 16 : 598; these upper limits are, however, comparable to the reported fluxes for BD + 16 :592. The stars BD + 16 :601 and BD + 16 :598 are somewhat fainter and of later spectral type than BD + 16 :592. The lack of detectable emission in the cooler Hyader dwarfs is probably just a selection effect due to the limited sensitivity of IUE exposures. Time variations in stellar activity may also play a role in determining the detectability of such emission.

b) Long Wavelength Spectra (1900-3200 Å)

LWR spectra of 71 Tau, BD + 15:640 and 70 Tau were taken to search for the presence of Mg II h and k chromospheric emission reversal. We observed Mg II emission lines in BD + 15:640 and 70 Tau, but failed to detect them in 71 Tau (Figure 2). This apparent absence of Mg II emission in the 71 Tau spectrum could be due to rotational smearing of the weak emission line in the core of the strong absorption line: 71 Tau has an apparent rotational velocity of 192 km/sec, leading to a 1.9Å broadening of an emission line at ~ 2800Å. The fluxes in the observed h and k emission lines are reported in Table 3. The Mg II "k3" absorption features (Fig. 2) are probably interstellar (Bohm-Vitense 1981).

Weiler and Oegerle (1979) have derived relations for the visual magnitude and the Mg II k emission line luminosity as a function of the Mg II k emission line width similar to the Wilson-Bappu relation. We applied their relations to the two stars for which we had positive detection of Mg II emission. We find that BD + 15 :640 has about the line width and Mg II k luminosity expected for its spectral type; 70 Tau has a greater width and higher luminosity than expected, but within the uncertainties in the observations.

Following the discussion of Linsky and Ayres (1978), we may estimate chromospheric radiative losses through the Mg II resonance line core. In the sun, the Mg II lines contribute approximately 30% of the total radiative loss, and this ration should not vary much, at least for solar type objects. Therefore, we may derive an upper limit for the radiative losses in 71 Tau of 10^7 ergs/cm^2/sec. For BD + 15:640 and 70 Tau, these radiative losses are approximately 1.3×10^7 ergs/cm^2/sec and 1.1×10^7 ergs/cm^2/sec, respectively. These numbers imply that BD + 15:640, 70 Tau and 71 Tau are transforming 1.4×10^{-4}, 1.3×10^{-4} and less than 6×10^{-5} of their total luminosity (as measured by σT_{eff}^4) into mechanical energy, compared to 5.5×10^{-5} for the quiet sun.

III. DISCUSSION

a) Constraints on Chromospheric and Transition Region Parameters

For optically thin lines which are collisionally excited, the power (erg/sec) emitted in a line λ is given by:

$$I_\lambda = \int n^2 \, G_\lambda(T) \, d^3V \qquad (1)$$

where n is the electron density and G_λ is the excitation function of the line. Since G_λ is usually a sharply peaked function, the integral may be approximated by:

$$I_\lambda = 0.7 \, G_\lambda \, (T_\lambda) \, EM \, (T_\lambda) \qquad (2)$$

where T_λ is the temperature at which G_λ peaks, and $EM(T_\lambda)$ is the effective emission measure at that temperature (e.g., Pottasch 1964). We have applied Equation (2) to the four hottest lines in the IUE spectra for which the assumption of being optically thin is presumably valid. Table 5 gives the emission measures (E.M.) for the four stars for which we have positive line identifications and for the Quiet Sun. If we assume that (as is the case for the Sun), the emission originates from an isobaric, planar transition region, then the emission measure of a particular line λ, may be approximated by:

$$EM_\lambda = (n_\lambda \cdot H_\lambda) \, (P_o \quad \Sigma) \, (2kT_\lambda)^{-1} \, (2\pi R^2) \qquad (3)$$

where n_λ is determined by the perfect gas law $n_\lambda = P_o/2kT_\lambda$; Σ is the fraction of the stellar surface emitting this line; R is the stellar radius, and H_λ is the scale height defined by the temperature gradient, T ds/dt, at temperature T_λ. If we further assume that the transition region plasma is static, then the temperature scale height can be determined from the requirement that the radiative losses be sufficient to dissipate the conductive flux through the transition region (Vesecky, Antiochos and Underwood 1979):

$$H \simeq 10^{-3}\ n^{-1}\ T^{7/4}\ \Lambda(T)^{-1/2} \tag{4}$$

where $\Lambda(T)$ is the radiative loss function for optically thin emission (Cox and Tucker, 1969), Raymond, Cox and Smith 1976). In our calculations, we have approximated the radiative loss function with the following functional form:

$$\Lambda(T) = \begin{cases} 10^{-19}\ T^{-1/2}, & 10^5 \leq T \leq 2 \times 10^7 K \\ 3.5 \times 10^{-27}\ T^{1/2}, & T \geq 2 \times 10^7 K \end{cases} \quad \text{ergs cm}^3/\text{sec} \tag{5}$$

Combining Equations (3) and (4) an expression can be derived for the product of pressure and stellar coverage at temperature T_λ:

$$(P_o\ \ \Sigma)_\lambda = 2.76 \times 10^{-13}\ (2\pi R^2)^{-1}\ T_\lambda^{-3/4}\ \Lambda(T_\lambda)^{1/2}\ EM_\lambda \tag{6}$$

We expect Equation (6) to be valid only for lines formed above the chromosphere. In the chromosphere, the dominant radiative losses are due

to optically thick emission; therefore, Equation (4) does not hold for $T \lesssim 3 \times 10^4 K$. In addition, it is not likely that a static isobaric model is valid for the chromosphere. It is certainly not valid for the solar chromosphere. As a test of the model, we computed $(P_o\ \Sigma)$ using Equation (6) for the observed C IV and N V lines from 70 Tau. The results agree to better than 3%, which is well within the uncertainties in our data.

As stated previously, we assume P_o to be constant over the transition region. In addition, we will assume the stellar coverage Σ to be the same in the transition region (where C IV is formed) and at the base of the corona; hence:

$$(P\ \ \Sigma)_{C\ IV} \simeq (P_o\ \Sigma)_{N\ V} \simeq (P_o\ \Sigma)_{cor} \qquad (7)$$

This is valid only as a first approximation since, if the emission originates from active region loops, as in the Sun, we expect that the loop cross-section varies from the transition region to the corona. However, for simplicity, we will assume a constant loop cross-section. Using Equation (7) the temperature at the base of the corona can be derived, viz:

$$\frac{G_x\ (T_{cor})}{\Lambda^{1/2}(T_{cor})}\ T_{cor}^{3/4} = 2.76 \times 10^{-13}\ \frac{L_x}{2\pi R^2} \cdot \left(\frac{1}{P_o\ \ \Sigma}\right) \qquad (8)$$

where $(L_x\ /\ 2\pi R^2)$ is simply the X-ray surface flux, G_x is the emissivity of the plasma in the X-ray band observed, and $(P_o\ \Sigma)$ is obtained from the UV observations, Equation (6). We may now derive an upper limit on Σ due to the fact that the size scale of the coronal emission must be less than

or of the order of the gravitational scale height:

$$\Sigma \lesssim \Sigma_{max} = 3 \times 10^{26} T_{cor}^{-7/4} \Lambda(T_{cor})^{1/2} \frac{(P_o \quad \Sigma)}{g} \qquad (9)$$

where g is the stellar surface gravity, and can be obtained from Allen (1973).

Note that there are certain limitations inherent in Equations (7) and (8). First, there is the assumption that Σ is the same for the corona and transition region. Second, there is the implicit assumption that the X-ray and UV observations are simultaneous. Unfortunately, this is not the case with our data sets since there is approximately a six month interval between the Einstein and the IUE observations. Finally, the model strictly applies to only a single coronal loop so that a unique T_{cor} and a unique P_o are possible. If, as is more likely, the emission is due to a collection of active region loops with different T_{cor} and P_o, then the values determined by Equations (7) and (8) will represent some "average" loop. As long as the range of variation of T_{cor} and P_o is not too large, these average values determined by our model will be physically significant. However, if, for example, the X-ray emission is due to a single very hot, dense loop whereas the UV emission is dominated by cool, low pressure loops, then our results will not be valid.

For the case of the Sun, Equations (8) and (9) do yield reasonable values. Assuming a moderately active Sun with an X-ray luminosity of $L_x = 10^{27.5}$ erg/sec and a coronal temperature of about $T_{cor} = 3 \times 10^6$ K in the active regions, then Equation (8) implies that $P_o \Sigma = 5.2 \times 10^{-2}$ dynes/cm^2.

Using Equation (9) the maximum value of the solar surface covered by active regions is $\Sigma_{max} \simeq 2\%$, implying a minimum pressure in the transition region of $P_{o\ min} = 2.5$ dynes/cm^2 and, therefore, an active region density at the base of the corona of $n_{cor} = 3 \times 10^9$ cm^{-3}, which agrees with observations.

We have performed the analysis described above on the four stars for which we have definite line identifications. Table 6 lists the values of the coronal parameters derived for these stars and, for comparison, a moderately active Sun with $L_x = 3 \times 10^{27}$ erg/sec. The errors on these results are probably quite large, at least a factor of two, due to the many uncertainties in the data and the model. However, they do provide a critical test of the hypothesis that the emission from these stars is due to a solar-like corona and transition region. The two F stars (BD + 15:640 and 70 Tau) tend to have similar characteristics: cooler coronae, larger "coverage" and, hence, smaller densities than the two G Hyades dwarfs. On the other hand, the two G stars (BD + 14:693 and BD + 16:592) are very dissimilar: while BD + 16:592 seems to be similar to the active Sun, BD + 14:693 has a very hot corona ($>10^7$K) and a very small coverage ($\sim$0.2%) leading to high densities especially in the transition region. Such a small coverage would be appropriate for a star in a flaring state. However, the X-ray observations did not indicate any time variability which could be associated with a flare, although the location of this star close to the ribs of the IPC makes the interpretation difficult.

Although BD + 14:693 has low values for the ultraviolet fluxes compared to its high X-ray flux, it may still be compatible with a static

loop model if temporal variations are considered. Several months elapsed between the X-ray and Ultraviolet observations, so that cyclic variation, similar to the Sun's may have occurred. Also if, indeed, the fraction of stellar surface covered by active regions is so small, then we have to take into account the "rotational modulation". We do not have any measurements of rotational velocity for BD + 14:693; however, the average value of $v_{rot} \simeq 9$ km/sec for Hyades solar-type dwarfs (Stern et al. 1981), Zolcinski, 1981) implies that any single active region rotates in about 5 days, a time which is much longer than any X-ray or Ultraviolet observation. Therefore, the case of a single active region is not excluded and it would be impossible to associate the X-ray flux and the Ultraviolet flux unless they were determined simultaneously.

It is of interest to consider the relation between coronal emission and stellar rotation. Only three stars out of four had their rotational velocities measured, (see Table 1). Neglecting the anomalous case of BD+14:693, it seems that the coronal temperatures deduced from the static conductively heated loop model are essentially independent of stellar rotation. Considering the average characteristics of the Hyades stars, it seems rather that the emission measure increases with increasing rotational velocity although our data are not reliable enough to suggest a particular functional dependence. From Table 6 it appears that the main difference between the Sun, (which is an old, slow rotator), and the Hyades stars (young, fast rotators) is in the area covered by active regions, i.e., Σ_{max}, and not in the physical characteristics of these regions. However, it should be emphasized that we are able to obtain only an upper limit on Σ. If, instead,

one assumes that Σ is the same for the Sun and the Hyades, then it is the coronal pressure that increases with increasing rotational velocity.

b) Differential Emission Measure

The differential emission measure used in Equation 2 is defined as (e.g., Antiochos, 1980):

$$EM \equiv A\, n^2\, H \qquad (10)$$

where A is the area of the emitting source. Assuming, as before, a static, isobaric loop with constant area, we may obtain a relation for EM as a function of temperature only:

$$EM(T) \propto T^{3/4}\, \Lambda\, (T)^{-1/2} \qquad (11)$$

where we have used Equation (4). In most cases of interest, we will have $10^5 \leq T < 2 \times 10^7$ K and we may apply the first expression in Equation 4 to obtain:

$$EM(T) \propto T \qquad (12)$$

This result applies only to an atmosphere containing a single loop or identical loops; however, the observed emission measure may be due to the contributions of loops at different temperatures. If all the loops are compatible with the static model, then the observed value of the slope will be less than the unity since no individual loop contributes a slope steeper than unity (Antiochos, 1980). Hence, we may deduce the temperature dependence of the emission measure for $T \geq 10^5$ K to be $EM \propto T^{\delta}$ where $\delta \leq 1$.

The solar emission measure is observed to agree with this prediction. In the range $10^5 \lesssim T \lesssim 10^6$, δ is observed to be less than unity (Raymond and Doyle, 1981). A minimum is observed in the emission measure at $T \simeq 10^5$, with a subsequent increase in EM(T) for cooler temperature, i.e., $\delta < 0$ for $T < 10^5$. Small or negative values of δ may be readily understood as the effect of a collection of loops at different temperatures. In addition, the radiative loss function turns over and becomes an increasing function of T for $T \lesssim 10^5$. From Equation (11) we note that this also has the effect of decreasing δ, (for $T \lesssim 10^5$).

We have computed for BD+15:640, 70 TAU, BD+14:693 and BD+16:592 the emission measures at those temperatures in the transition region where the ions of C II, Si IV AND N V are most abundant. The results are given in Table 5. We also list the X-ray emission measures obtained from the Einstein observations. For comparison, the values of the emission measures of the Quiet Sun, with $L_x = 3 \times 10^{26}$ erg/sec are given in Table 5, as well.

In order to compare the slopes of the emission measures, we normalized them by the emission measure at $T = 10^5$K, namely, $EM_{C\ IV}$. The choice of C IV as a normalization factor is purely practical: it is the only emission line for which we have positive identifications in the four Hyades stars. The results are plotted in Figure 3. It is to be noted that these curves are not model independent at the higher temperatures. The calculation of the coronal emission measure involves the knowledge of T_{cor} deduced in Section III (a) using the static loop model. Hence, the slope of the differential emission measure between $\sim 10^5$K and T_{cor} equals unity, since this result is implicitly assumed in the static loop model.

We expect the actual slopes to be somewhat less than unity (as in the Sun) due to the contribution of cool loops. Hence, our estimate for T_{cor} is probably only a lower limit on the true coronal temperature. Figure 3 shows also the differential emission measure for the Quiet Sun, which is model independent throughout the temperature range since T_{cor} is well determined observationally.

The first striking feature that can be seen in Figure 3 is that $EM_{C\ IV}$ is minimum in all stars. This is a true minimum in the case of the Sun; however, the curves may be misleading in the case of the Hyades stars. We have only four points to construct the differential emission curves, in addition, some of these points are only upper limits (identified by arrows in Figure 3). In the extreme case of BD+16:592, we have upper limits for all points except C IV and the X-rays. Therefore, the minimum may lie anywhere below $T \simeq 10^5$K.

Of more interest are the results for the region below 10^5K since these are model independent. As is evident from Figure 3, the differential emission measure curves in the temperature range 3×10^4 K < T < 10^5K are very similar for the Sun and the Hyades stars (within the observational errors) so that EM (T) $\propto$ T^{-2}. We can even extend this similarity up to T = 2×10^5, K for 70 Tau and the Quiet Sun. Doschek et al (1978) have obtained the same result for α Aur, HR1099, λ And, ε Eri and for several very different regions of the solar atmosphere (Quiet Sun, Coronal Hole, active region, flares). It appears, therefore, that while the absolute value of the emission measure may change for different stars, (by a factor of 30 or more), the shape of emission measures for 3×10^4 K < T < 10^5K seems to be

the same, at least, for different regions of the Sun, the Hyades stars observed and the stars mentioned above. We believe that this is an important result and that more observations are clearly needed to determine whether this effect holds for other stars, as well.

The observed form of EM(T) for $T < 10^5$, (i.e., $\delta \simeq -2$), does not seem to be compatible with the static loop model. Pallavicini et al. (1981) have performed a detailed comparison of solar observations with the standard static models, and found that they could not reproduce the observed rise in EM(T) at low temperatures. Several explanations are possible. One is that the coronal heating mechanism, (whatever that may be), becomes greatly enhanced at low temperature. However, as pointed out by Craig, McClymont and Underwood (1978), the differential emission measure predicted by the static model is essentially independent of the coronal heating function, unless one assumes a highly artificial form for this heating. Hence, we consider this possibility to be unlikely. Another explanation is that it is due to the effect of a collection of static loops with a particular distribution of loop parameters, i.e., area, P_o, T_{cor}, etc. We also consider this to be unlikely since there is no apparent reason why the same distribution of loops should occur in vastly different regions of the sun and on stars of different types. The most likely possibility is that the static model is not valid in this temperature range and that the form of the differential emission measure is due to the effect of mass motions. We intend to explore this possibility in a subsequent paper.

IV. SUMMARY OF THE ULTRAVIOLET OBSERVATIONS

The results of this paper may be summarized as follows:

1. Although the IUE sensitivity limit did not allow us to detect

emission lines in three stars, we confirm the presence of chromospheres and transition regions in BD+15:640, 70 TAU, BD+14:693 and BD+16:592, already postulated through their X-ray emission.

2. We have observed three stars with the IUE long wave-length camera and estimated the chromospheric radiative losses in BD+15:640 and 70 TAU to be roughly twice as large as in the Sun. The upper limit of the chromospheric radiative losses of 71 TAU is of the order of the Sun's value.

3. Assuming a plane-parallel transition region, one finds that the power emitted by an optically thin line is proportional to the product of the pressure and the emitting fraction of stellar surface. Assuming, in addition, a static conductively heated loop model, one may combine the ultraviolet and soft X-ray observations to derive an isothermal coronal temperature and to constrain the density, pressure and emitting fraction of the stellar surface. With the above assumptions, we find that BD+15:640, 70 TAU and BD+16:592 are all consistent with a static conductively heated loop model. However, BD+14:693 is not compatible with such a model unless strong temporal variations in its UV and X-ray emission are postulated.

4. We have plotted the differential emission measure as a function of temperature for the four stars mentioned above. While the absolute values of the emission measures vary by a factor of 30 between the Quiet Sun and the two G Hyades dwarfs, their slopes are fairly similar: they exhibit a solar-like minimum between 3×10^4 K $\lesssim$ T $\lesssim$ 2×10^5 K. For temperatures lower than T < 10^5K, the slopes are identical within the error of measurements (EM (T) $\propto T^{-2}$). For T > 10^5K, the possible contribution of cool loops implies that the estimated coronal temperature derived is a lower limit.

ACKNOWLEDGEMENTS

We thank A. Boggess and the staff of the IUE Observatory for their assistance in the acquisition of these data. We are indebted to A. Lane, T.R. Ayres, R.E. Stencel, P. Bornmann and L. Caroff for their help in using the computer facilities at the Jet Propulsion Laboratory (Pasadena, Calif.), the Joint Institute for Laboratory Astrophysics (Boulder, Colo.) and the NASA-Ames Research Center (Mountain View, Calif.). We would like to thank the referee for helpful comments. In addition, M-C. Zolcinski would like to express her genuine appreciation to J.L. Linsky and R.E. Stencel for their help and guidance in the ultraviolet data analysis. M-C. Zolcinski and A.B.C. Walker, Jr., were supported by NASA grants NSG 5131 and NSG 5417; S.K. Antiochos was supported by NASA grants NGR-05-020-668, NGL-05-020-272 and NAGW-92; R.A. Stern was supported by NASA grant NAS 7-100.

REFERENCES

Allen, C. W., 1973, "Astrophysical Quantities", Athlone Press, London.

Antiochos, S. K., 1980, Ap. J., 241, 385.

Ayres, T. R., Marstad, N. C., Linsky, J. L., 1981, Ap. J., 247, 545.

Barnes, T., Evans, D., 1976, M. N. R. A. S., 174, 489.

Boggess, A., et al., 1978a, Nature, 275, 372.

Boggess, A., et al., 1978b, Nature, 275, 377.

Bohlin, R. C., Holm, A. V., Savage, B. D., Snijders, M. A. J., Sparks, W. M., 1980, Astr. Ap., 85, 1.

Bohm-Vitense, E. 1981, Ap. J., 244, 504.

Burton, W. M., Ridgeley, A., 1970, Solar Phys., 14, 3.

Cox, D. P., Tucker, W. H., 1969, Ap. J., 157, 1157.

Craig, I. J. D., McClymont, A. N., and Underwood, J. H. 1978, Astr. Ap., 70, 1.

Doschek, G. A., Feldman, U., Mariska, J. T., Linsky, J. L., 1978, Ap. J., 226, L35.

Doschek, G. A., Feldman, U., Van Hoosier, M. E., Bartoe, J-D., F., 1976, Ap. J., Suppl., 31, 417.

Dupree, A. K., 1981, "Solar Phenomena in Stars and Stellar Systems", (Eds. R. M. Bonnet and A. K. Dupree), Reidel, Holland.

Holm, A., 1979, NASA IUE Newsletter No. 7, 27.

Linsky, J. L., Worden, S. P., McClintock, W., and Robertson, R. M. 1979, Ap. J. Suppl., 41, 47.

Linsky, J. L., 1981, "Solar Phenomena in Stars and Stellar Systems", (Eds. R. M. Bonnet and A. K. Dupree), Reidel, Holland.

Linsky, J. L., Ayres, T. R., 1978, Ap. J., 220, 619.

Pottasch, S. R., 1964, Space Sci. Rev., 3, 816.

Raymond, J. C., Cox, D. P., Smith, B. W., 1976, Ap. J., 204, 290.

Raymond, J. C., Doyle, J. G., 1981, preprint, (submitted to Ap. J.).

Stern, R. A. Zolcinski, M-C., Antiochos, S. K., Underwood, J. H., 1981, Ap. J., 244, 647.

Vaiana, G. S., et al., 1981, Ap. J., 245, 163.

Vesecky, J. F., Antiochos, S. K., Underwood, J. H., 1979, Ap. J., 233, 987.

Walter, F. and Bowyer, S., 1981, Ap. J., 245, 671.

Weiler, E. J., Oegerle, W. R., 1979, Ap. J. Suppl., 39, 537.

Zolcinski, M-C., 1981, Stanford Institute for Plasma Research Report #843, Stanford, California.

Table I STELLAR PARAMETERS

71 TAU		BD+15:640	70 TAU	BD+14:693	BD+16:592	BD+15:598	BD+16:601
Sp	F0 V	F5 V	F7 V	G1 V	G1 V	G5 V	G6 V
V	4.50	6.51	6.46	7.62	7.80	8.06	8.12
B - V	0.25	0.42	0.49	0.60	0.60	0.63	0.66
V - R	0.27	0.40	0.45	0.52	0.52	0.54	0.56
ϕ	0.66	0.34	0.38	0.26	0.24	0.22	0.22
v sin (i) (km/sec)	192	53	15	-	6	-	-
T_{eff} (K)	7450	6440	6180	5870	5870	5770	5660
log(g) cm/sec^2	4.25	4.3	4.3	4.4	4.4	4.44	4.5

Table 2 SUMMARY OF IUE OBSERVATIONS

Star	Image	Day (Year 1980)	Begin time (UT)	Exposure (min.)
71 TAU	SWP 9855	234	14.47*	3
			14.57	3
	SWP	236	09.48	20
	LWR 8591	236	09:38	6
	LWR 8572	234	14:19	20
BD+15:640	SWP 9856	234	16:10	96
	SWP 9875	236	10:56	120
	LWR 8573	234	15:35	30
70 TAU	SWP 9877	236	17:09	38
	SWP 9853	234	02:36	240
	LWR 9871	234	06:44	30
	LWR 8592	236	16:35	28
BD+14:693	SWP 9876	236	13:28	180
BD+16:592	SWP 9854	234	07:23	400
BD+16:598	SWP 9614	209	16:44	186
BD+16:601	SWP 9612	209	12:46	60
	SWP 9613	209	14:15	120
	SWP 9873	236	02:37	390

*small aperture

Table 3 SUMMARY OF OBSERVED EMISSION LINE FLUXES AT EARTH (ergs/cm^2/sec)

λ (A)	Ion	71 TAU	BD+15:640	70 TAU	BD+14:693	BD+16:592	BD+16:598	BD+16:601
1240	N V (1)	< 1(-12)	< 4(-14)	2.8(-14)	< 3(-14)	< 3(-14)	< 5.5(-14)	< 3(-14)
1305	O I (2)	< 1(-12)	< 4(-14)	2.7(-14)	< 3(-14)	< 3(-14)	< 4.4(-14)	< 3(-14)
1335	C II (1)	< 1(-12)	7(-14)	5.3(-14)	5.8(-14)	< 3(-14)	< 5.5(-14)	< 3(-14)
1394	Si IV (1)	< 1(-12)	< 4(-14)	4(-14)	5.0(-14)	< 3(-14)	< 5.5(-14)	< 3(-14)
1482	S I (3+4)	< 1(-12)	< 4(-14)	< 2(-14)	7(-14)	< 3(-14)	< 5.5(-14)	< 3(-14)
1549	C IV (1)	< 2(-12)	1.6(-13)	1.4(-13)	7.6(-14)	4(-14)	< 5.5(-14)	< 3(-14)
1561	C I (3)	< 2(-12)	6.5(-14)	< 2(-14)	6.8(-14)	< 3(-14)	< 5.5(-14)	< 3(-14)
1657	C I (2)	< 2(-12)	8.7(-14)	< 3(-14)	< 4(-14)	< 3(-14)	< 5.5(-14)	< 3(-14)
1705,10	Fe II	satur.	< 2(-13)	1.5(-13)	< 4(-14)	< 2(-14)	< 5.5(-14)	< 5(-14)
1817	Si II (2)	satur.	< 2(-13)	< 3.5(-14)	5.9(-14)	3.5(-14)	< 5.5(-14)	< 5(-14)
2796	Mg II k	< 5(-12)	1.5(-12)	1.6(-12)	---	---	---	---
2803	Mg II h	< 3(-12)	1.2(-12)	1.2(-12)	---	---	---	---
Soft X-rays		4.0(-12)	1(-12)	1.2(-12)	4.0(-12)	5.2(-13)	8.2(-13)	1.3(-12)

Table 4 SUMMARY OF LINE SURFACE FLUXES (ergs/cm^2/sec)

λ (Å)	Ion	BD+15:640	70 TAU	BD+14:693	BD+16:592	Quiet Sun
1240	N V (1)	< 6(4)	3.3(4)	< 7.6(4)	< 8.9(4)	8.6(2)
1305	O I (2)	< 6(4)	3.2(4)	< 7.6(4)	< 8.9(4)	4.0(3)
1335	C II (1)	1.0(5)	6.3(4)	1.5(5)	< 8.9(4)	4.6(3)
1394	Si IV (1)	< 6(4)	< 4.8(4)	1.3(5)	< 8.9(4)	1.7(3)
1482	S I (3+4)	< 6(4)	< 2.4(4)	1.8(5)	< 8.9(4)	5.3(2)
1549	C IV (1)	2.4(5)	1.7(5)	1.9(5)	1.2(5)	5.8(3)
1561	C I (3)	9.6(4)	< 2.4(4)	1.7(5)	< 8.9(4)	2.0(3)
1657	C I (2)	1.3(5)	< 3.6(4)	< 1(5)	< 8.9(4)	5.3(3)
1705, 10	Fe II	< 3(5)	1.8(5)	< 1(5)	< 5.9(4)	------
1817	Si II (2)	< 3(5)	< 4.2(4)	1.5(5)	1.0(5)	1.0(4)
2796	Mg II k	2.2(6)	1.9(6)	-----	-----	6.0(5)
2803	Mg II h	1.8(6)	1.4(6)	-----	-----	4.5(5)
Soft X-rays		1.5(6)	1.4(6)	1.0(7)	1.5(6)	------

Table 5 EMISSION MEASURES (cm^{-3})

	$EM_{C\ II}$	$EM_{Si\ IV}$	$EM_{C\ IV}$	$EM_{N\ V}$	EM_{X}
BD+15:640	1.24(51)	< 2.49(50)	6.55(49)	< 1.27(50)	6.5(50)
70 TAU	6.79(50)	< 1.74(50)	4.06(49)	6.08(49)	7.4(50)
BD+14:693	1.42(51)	4.12(50)	3.98(49)	< 1.23(50)	1.4(52)
BD+16:592	< 8.43(50)	< 2.83(50)	2.51(49)	< 1.44(50)	1.0(51)
QUIET SUN	3.95(49)	4.89(48)	1.10(48)	1.28(48)	4.0(48)

Table 6 MODEL PARAMETERS

Star	$P_o \cdot \Sigma$ (dynes/cm^2)	T_{cor} (K)	Σ_{max}	$P_{o\ min}$ (dynes cm/^{2})	$n_{o\ min}$ at $T=10^5$K, cm^{-3}	$n_{cor,min}$ at $T=T_{cor}$, cm^{-3}	$H_{o\ max}$ (cm)
BD+15:640	1.3	9.7(5)	1	1.3	4.7(10)	4.8(9)	3.8(9)
70 TAU	0.9	1.9(6)	1	0.9	3.3(10)	1.7(9)	1.1(11)
BD+14:693	1.0	4.6(7)	2.3(-3)	4.35(2)	1.6(13)	3.4(10)	2.8(11)
BD+16:592	0.65	4.3(6)	1.3(-1)	5.0	1.8(11)	4.2(9)	8.6(10)
QUIET SUN	$\simeq$ 1(1-2)	1.6(6)	5.0(-2)	0.2	7.2(9)	4.5(8)	1.3(10)
MODERATELY ACTIVE SUN	5(2)	3.0(6)	2.0(-2)	2.5	9.0(10)	3.0(9)	9.9(9)

FIGURE CAPTIONS

Figure 1 IUE short wavelength spectra of the Hyades stars

Figure 2 IUE long wavelength spectra of three Hyades stars: the MG II h and k region

Figure 3 Differential emission measure for four Hyades stars and the Quiet Sun in units of $EM_{C\ IV}$ (emission measure at $T = 10^5 K$). Upper limits are indicated by triangles.

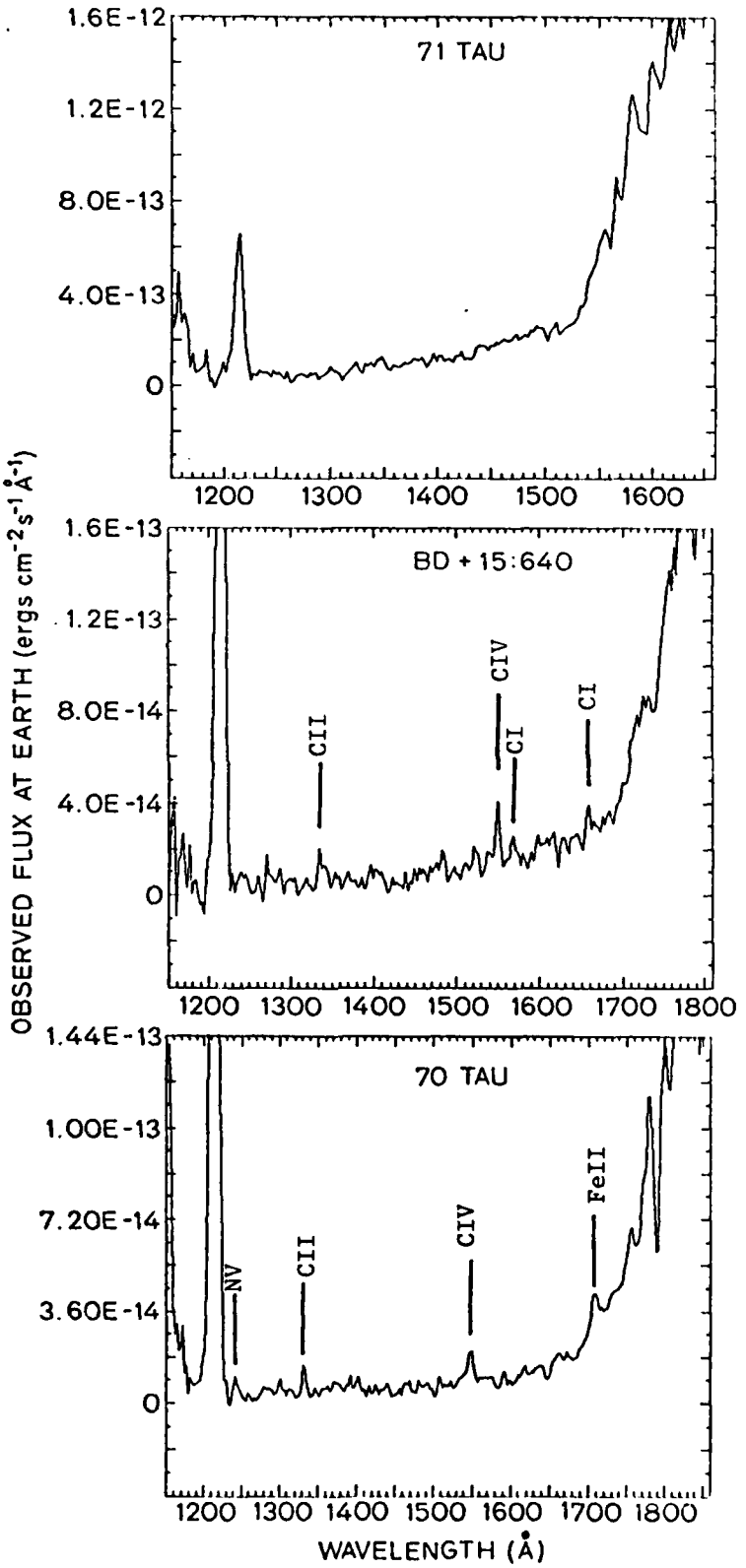
71 TAU
BD + 15:640
70 TAU
OBSERVED FLUX AT EARTH (ergs cm^{-2}s^{-1}Å^{-1})
WAVELENGTH (Å)
CII
CIV
CI
NV
FeII

Figure 1

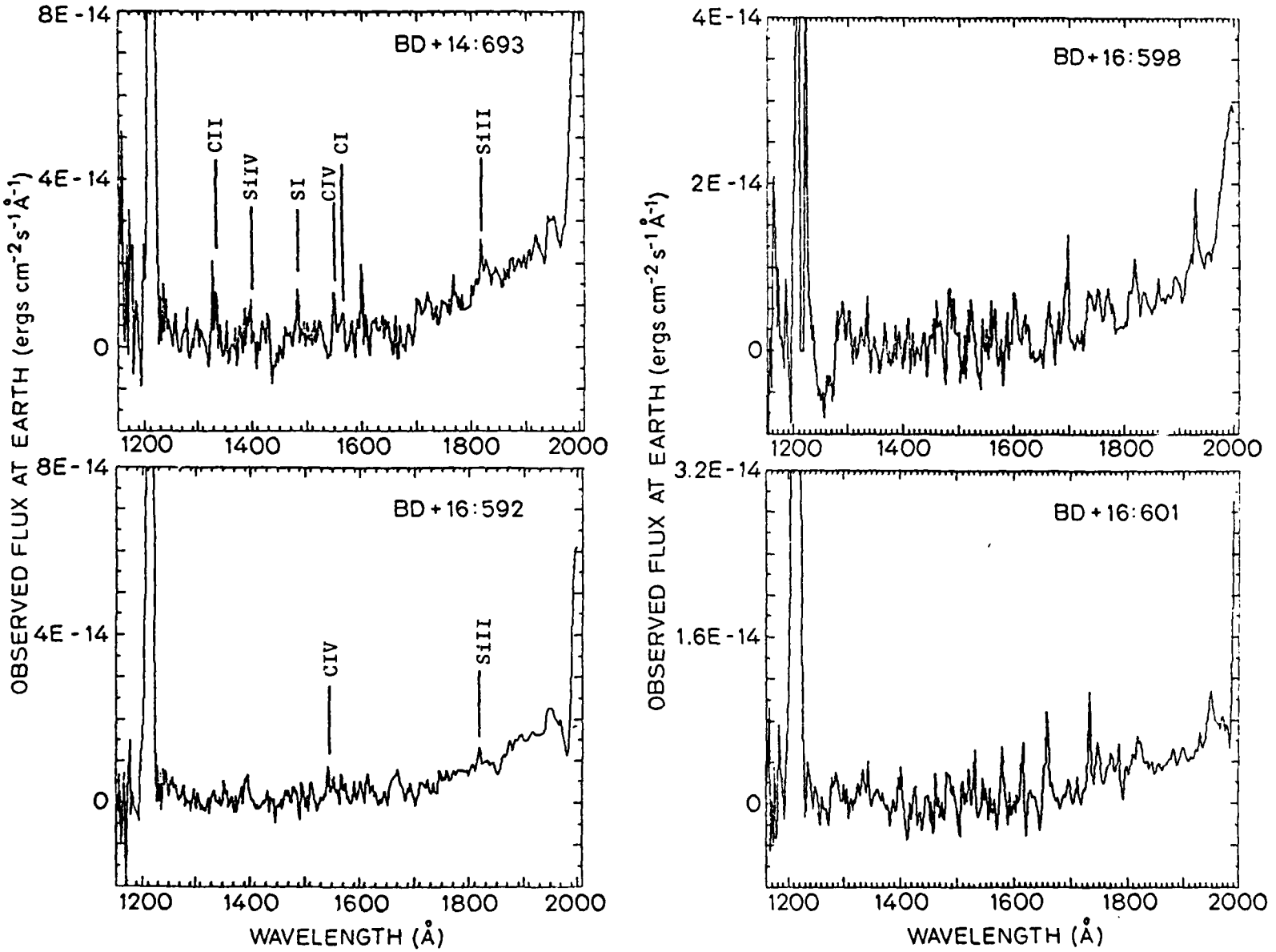
BD+14:693
CII
SiIV
SI
CIV
CI
SiII
BD+16:592
CIV
SiII
BD+16:598
BD+16:601
8E-14
4E-14
0
2E-14
3.2E-14
1.6E-14
1200
1400
1600
1800
2000
OBSERVED FLUX AT EARTH (ergs cm^{-2}s^{-1}Å^{-1})
WAVELENGTH (Å)

Figure 1

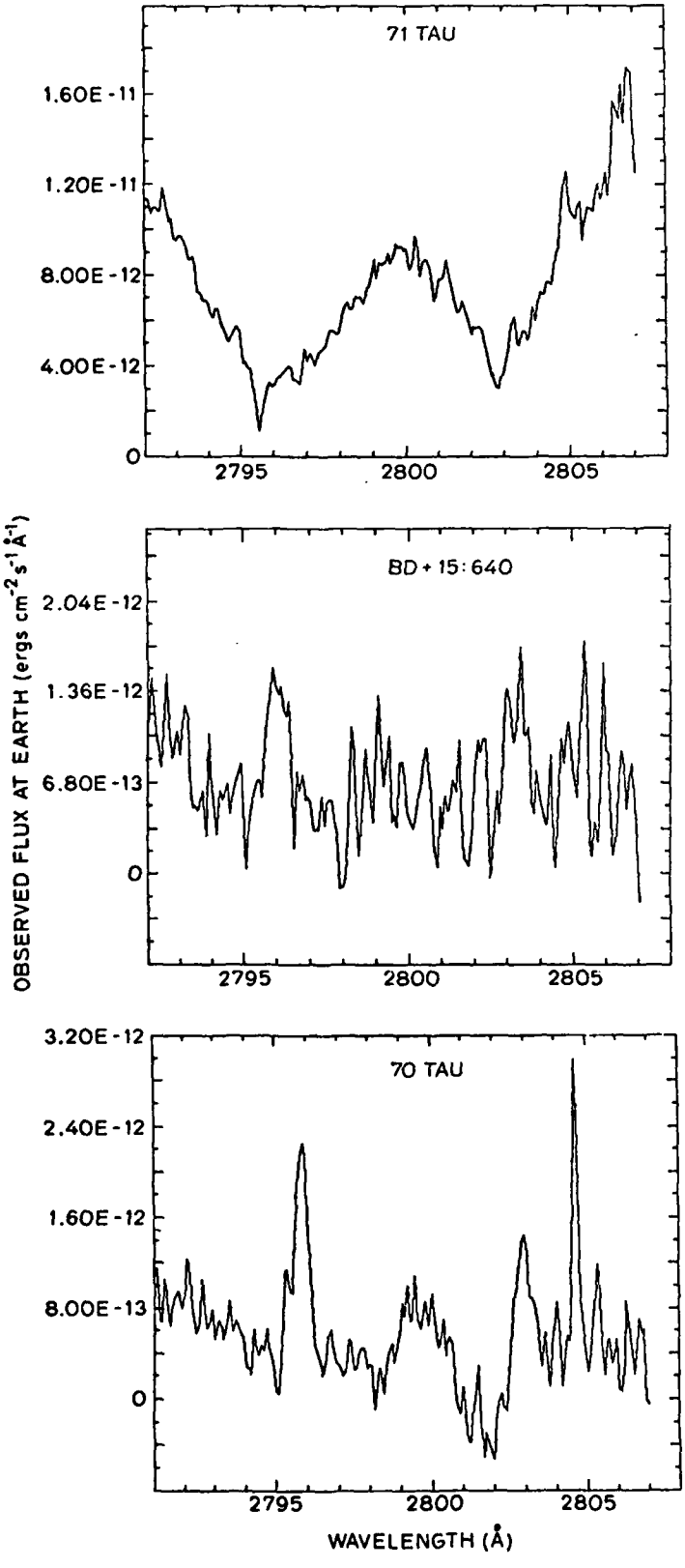
71 TAU
1.60E-11
1.20E-11
8.00E-12
4.00E-12
0
2795
2800
2805
BD+15:640
2.04E-12
1.36E-12
6.80E-13
0
2795
2800
2805
OBSERVED FLUX AT EARTH (ergs cm^{-2} s^{-1} Å^{-1})
70 TAU
3.20E-12
2.40E-12
1.60E-12
8.00E-13
0
2795
2800
2805
WAVELENGTH (Å)

Figure 2

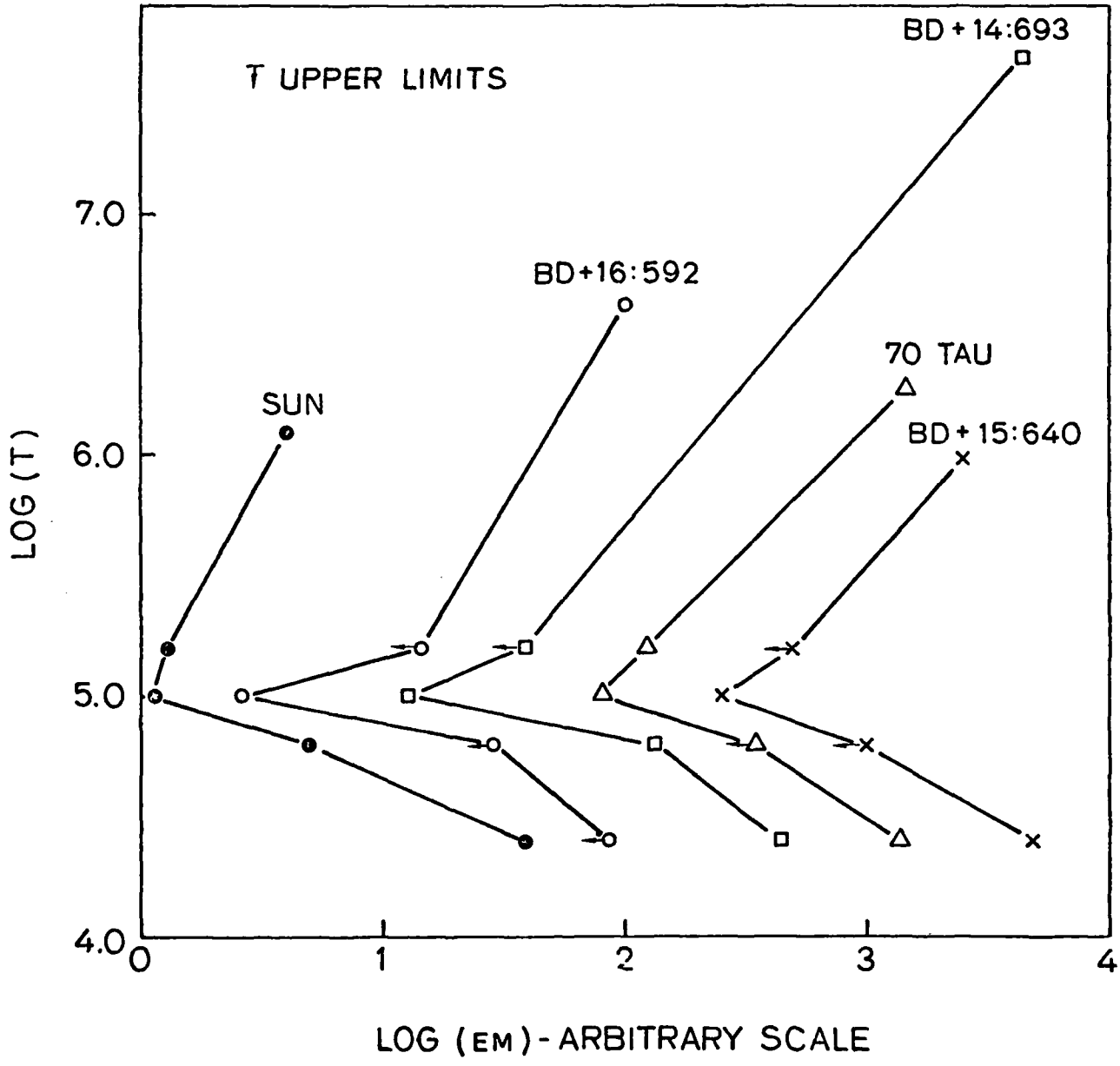
T UPPER LIMITS
BD + 14:693
BD+16:592
70 TAU
SUN
BD + 15:640
7.0
6.0
5.0
4.0
LOG (T)
0
1
2
3
4
LOG (EM) - ARBITRARY SCALE

Figure 3

M-C. S. Zolcinski, University of New Hampshire, DeMeritt Hall, Physics Dept., Durham, New Hampshire 03824.

S. K. Antiochos and A. B. C. Walker, Jr., Institute for Plasma Research, Via Crespi, Stanford University, Stanford, California 94305.

R. A. Stern, Jet Propulsion Laboratory, California Institute of Technology, 4800 Oak Grove Drive, Pasadena, California 91103.